



High-energy deuteron measurement with the CAPRICE98 experiment

M. Ambriola^a, S. Bartalucci^b, R. Bellotti^a, D. Bergström^c, M. Boezio^d, V. Bonvicini^d, U. Bravar^e, F. Cafagna^a, P. Carlson^c, M. Casolino^f, F. Ciaccio^a, M. Circella^a, C. N. De Marzo^a, M. P. De Pascale^f, N. Finetti^g, T. Francke^c, P. Hansen^c, M. Hof^h, J. Kremer^h, W. Menn^h, J. W. Mitchellⁱ, E. Mocchiutti^c, A. Morselli^f, J. F. Ormesⁱ, P. Papini^g, S. Piccardi^g, P. Picozza^f, M. Ricci^b, P. Schiavon^d, M. Simon^h, R. Sparvoli^f, P. Spillantini^g, S. A. Stephensⁱ, S. J. Stochaj^e, R. E. Streitmatter^j, M. Suffert^j, A. Vacchi^d, E. Vannuccini^g*, N. Zampa^d

^aUniversity of Bari and Sezione INFN di Bari, Bari, Italy

^bINFN – Laboratori Nazionali di Frascati, Frascati, Italy

^cRoyal Institute of Technology, Stockholm, Sweden

^dUniversity of Trieste and Sezione INFN di Trieste, Trieste, Italy

^eR. L. Golden Particle Astrophysics Lab, New Mexico State University, Las Cruces, NM, USA

^fUniversity of Roma “Tor Vergata” and Sezione INFN di Roma II, Rome, Italy

^gUniversity of Firenze and Sezione INFN di Firenze, Florence, Italy

^hUniversity of Siegen, Siegen, Germany

ⁱLaboratory for High Energy Astrophysics, NASA/Goddard Space Flight Center, Greenbelt, MD, USA

^jCentre des Recherches Nucléaires, Strasbourg, France

The CAPRICE98 balloon-borne instrument was flown on 28–29 May 1998 from Fort Sumner (New Mexico, USA). The detector configuration included the NMSU-WiZard/CAPRICE superconducting-magnet spectrometer equipped with a gas RICH, a silicon-tungsten calorimeter and a time-of-flight system. By combining the information from the spectrometer and the RICH, which was used as a threshold device, it was possible to separate ^2H from ^1H in the kinetic energy range from 12 to 22 GeV/n.

In order to estimate the proton background and the deuteron selection efficiency, an empirical model for the response of the instrument, based on the data collected in this experiment, was developed. The analysis procedure is described in this paper and the results on the absolute flux of ^2H and $^2\text{H}/\text{He}$ ratio are presented. These data on ^2H abundance represent the only measurements above 10 GeV/n.

1. Introduction

The CAPRICE98 balloon-borne experiment (Cosmic AntiParticle Ring Imaging Cherenkov Experiment, 1998) is the latest detector built and flown by the WiZard collaboration. The instrument configuration allowed several science objectives to be achieved, among which is the ^2H abun-

dance.

The presence of deuterons in cosmic rays is attributed to the interactions of cosmic rays with the interstellar medium during the propagation of the former through the Galaxy. Among other secondary nuclei, deuterons have considerably larger interaction mean free path than the escape mean free path from the Galaxy. As a result, they are a good probe to test propagation models. In spite

*Presenting author (vannucci@fi.infn.it)

of its scientific relevance not many measurements exist beyond ~ 1 GeV/n due to the difficult task of identifying deuterons out of the large background of protons.

2. The CAPRICE98 apparatus

The CAPRICE98 apparatus was designed to identify particles in the energy range from few hundreds MeV up to hundreds GeV. The instrument was composed of a drift chamber tracking system ($\sim 100 \mu\text{m}$ of spatial resolution) [1] placed inside the magnetic field generated by a superconducting magnet ($0.1 \div 2$ T inside the tracking volume) [2]. The tracking system provided 30 position measurements (18 in the bending view and 12 in the non bending one) from which the track deflection ($\eta = 1/R$, where R is the rigidity) was obtained after applying a least-squares fitting procedure [3]. The maximum detectable rigidity of the spectrometer in the CAPRICE98 configuration was 300 GV.

The instrument had three additional detectors and the information provided by these detectors, when combined with those of the spectrometer, enabled particle identification. Starting from the bottom of the payload there were a Si-W electromagnetic imaging calorimeter [5], a time-of-flight system and a gas RICH (Ring Imaging Cherenkov) detector [6].

The identification of high energy deuterons among the singly charged particles, which mostly consist of protons, was based on the information coming from the RICH used as a threshold device along with the rigidity measured by the spectrometer. The instrument consisted of a photosensitive MWPC, a 1 m tall radiator box filled with high purity C_4F_{10} gas (refractive index $n \sim 1.0014$) and a spherical mirror. For relativistic particles the number of detected photoelectrons was ~ 17 . The upper cathode plane of the MWPC was divided in pads so that a ring-like image was detected. The Cherenkov angle (θ_c) was reconstructed from the induced signal combined with the track information coming from the spectrometer. The achieved angular resolution was 1.1 mrad for relativistic particles, when the Cherenkov angle was 52.6 mrad.

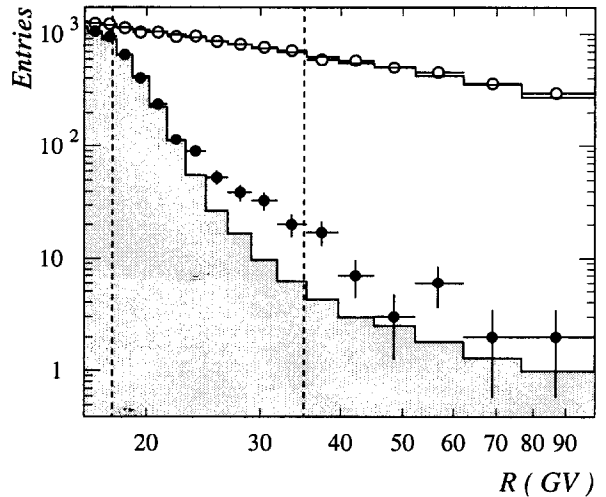


Figure 1. Distributions of the selected events as a function of the measured rigidity. Open circles: all selected events. Filled circles: events without a Cherenkov signal. Dashed lines: proton and deuteron Cherenkov threshold rigidities. Shaded area: simulated background distribution.

3. Data analysis

3.1. Proton and deuteron selection

The data set used for the ^2H analysis consisted of singly charged positive particles with a well reconstructed track in the spectrometer, and a having its trajectory contained in the sensitive volume of the detectors. A detailed description of the applied general selection criteria can be found in reference [7]² and references therein. The selected sample contained mainly protons and deuterons, with a negligible amount of particles of different type.

To select the deuterons we required that above the proton threshold rigidity (about ~ 18 GV) the event did not produce Cherenkov signal in the RICH. Fig. 1 (black circles) shows the number of selected events as a function of the rigid-

²Also available at <http://hep.fi.infn.it/PAMELA/tesi/tesi.html>

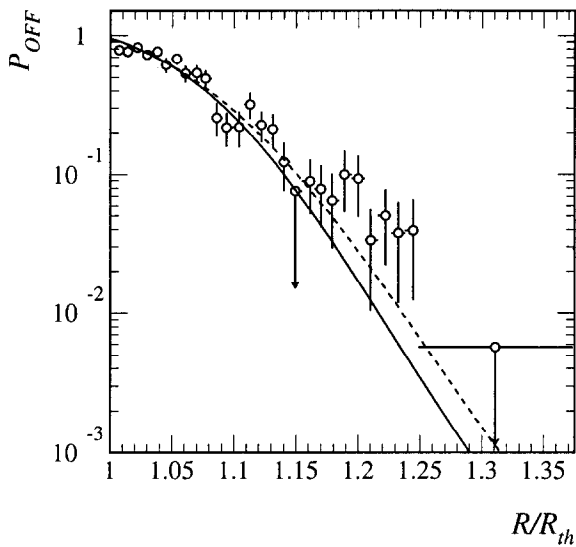


Figure 2. Probability P_{OFF} of detecting zero photoelectrons. Open circles: muons from ground data. Dashed curve: fit to experimental points. Solid curve: parameterization obtained after the correction for the spectrometer effect.

ity. Besides deuterons the selected sample contains proton events without a Cherenkov signal, which represent a non-negligible contamination.

Since the deuteron selection with the RICH cannot be cross-checked with any other detector, the background level was determined by means of a simulation. Our approach was to develop an empirical response model of the instrument based on characteristic quantities obtained from experimental data. The presence of proton events without a Cherenkov signal beyond the threshold is mainly due to the following two effects: 1) the probability of detecting zero photoelectrons above the Cherenkov threshold, which is different from zero even over threshold; 2) the uncertainty in the measured deflection. We needed to simulate both these effects in order to estimate the background level.

3.2. Probability of detecting zero photoelectrons

The probability of detecting no photoelectrons (P_{OFF}) by the RICH was estimated using muons from ground data.

The quantity P_{OFF} is related to the number of detected Cherenkov photoelectrons and, as a consequence, for particles of the same charge it does not depend on the particle type if expressed as a function of the velocity β , or equivalently η/η_{th} . The Cherenkov deflection threshold (η_{th}) for muons is about 10 times greater than that of protons. It follows that the spectrometer uncertainty, which is nearly constant in deflection, has a smaller effect for muons than for protons. Nevertheless, the spectrometer gives a small but finite effect, which is magnified due to the increase of the deflection uncertainty at low energy resulting from the multiple scattering inside the spectrometer. We thus inferred the probability P_{OFF} from the distribution of muons without a Cherenkov signal after the unfolding of the spectrometer response.

The unfolding procedure implied the knowledge of the low energy spectrometer resolution function, which is in the first approximation given by two independent contributions, related to respectively the spectrometer spatial resolution and to the multiple scattering effect. At high energy the latter contribution is negligible.

We constructed the low energy resolution function by means of a simulation based on the GEANT package. The simulation code took into account only the geometry and the materials of the spectrometer, so that the only physical process included was the multiple scattering. The simulated tracks were processed with the same track fitting algorithm used on experimental data. To the deflection value obtained from the above fitting routine, another contribution was then added. This contribution was generated according to the high energy spectrometer resolution function, which was obtained independently as described in section 3.3. We took the distribution of the resulting deflection as an estimate of the low energy spectrometer resolution function.

Fig. 2 shows the fraction of muons without a Cherenkov signal (open circles). The dashed

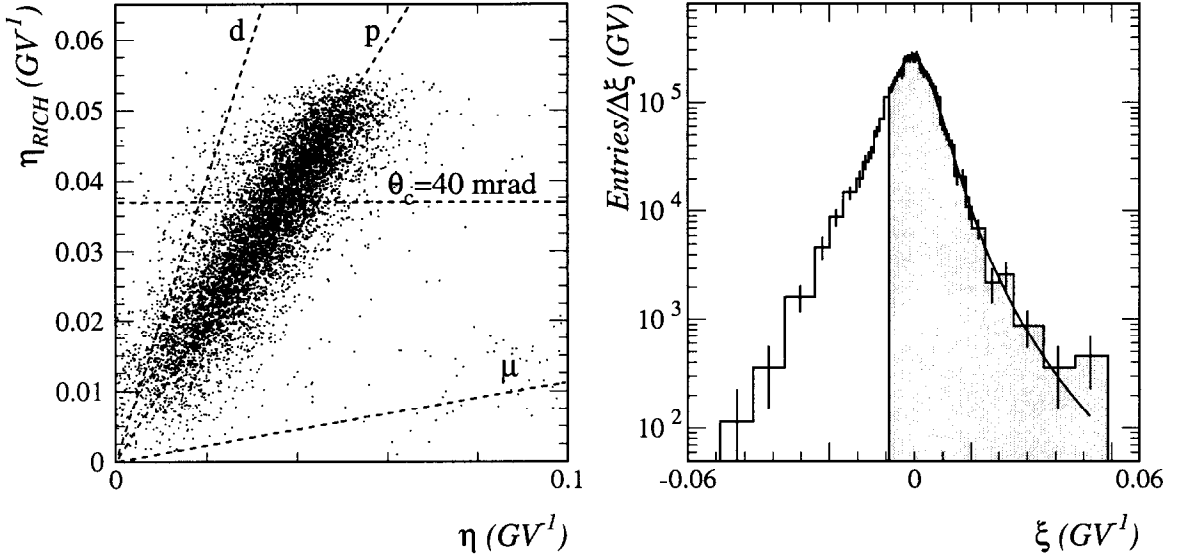


Figure 3. *Left plot*: deflection value derived from the reconstructed Cherenkov angle as a function of the deflection measured with the spectrometer. Inclined dashed lines: expected shape for deuterons, protons and muons. Horizontal dashed line: applied cut on the Cherenkov angle (the selected events are those above this line). *Right plot*: differential distribution of the number of selected particles as a function of the variable $\xi = \eta - \eta_{RICH}$. Solid curve: result of the fit, performed in the range highlighted by the shaded area. The χ^2 is ~ 1.1 , corresponding to a confidence level of $\sim 30\%$.

curve is a fit to the experimental points, while the solid line represents the result of the fit after the unfolding of the spectrometer response from the distribution of muons without a Cherenkov signal. We took this latter function as the best estimate of P_{OFF} at ground.

During the flight, the RICH performances changed due to different pressure and temperature conditions of the gas radiator, leading to a change in the number of emitted photoelectrons. The MWPC response remained instead unchanged. In order to compensate for this variation in flight, we scaled P_{OFF} using the observed number of detected photoelectrons relative to that on the ground.

3.3. High energy spectrometer resolution function

The spectrometer resolution function was obtained using protons from flight data.

We selected a sample of events with a well-defined ring in the RICH. We then calculated the deflection (η_{RICH}) from the reconstructed Cherenkov angle assuming a mass of a proton. In fig.3 (left plot) this quantity is plotted as a function of the deflection measured with the spectrometer.

The high energy spectrometer resolution function was derived from the distribution of the variable $\eta - \eta_{RICH}$. This distribution is in fact the convolution of the spectrometer resolution function and the deflection resolution function of the RICH. In order to minimize the RICH uncertainty and the contamination of particles other

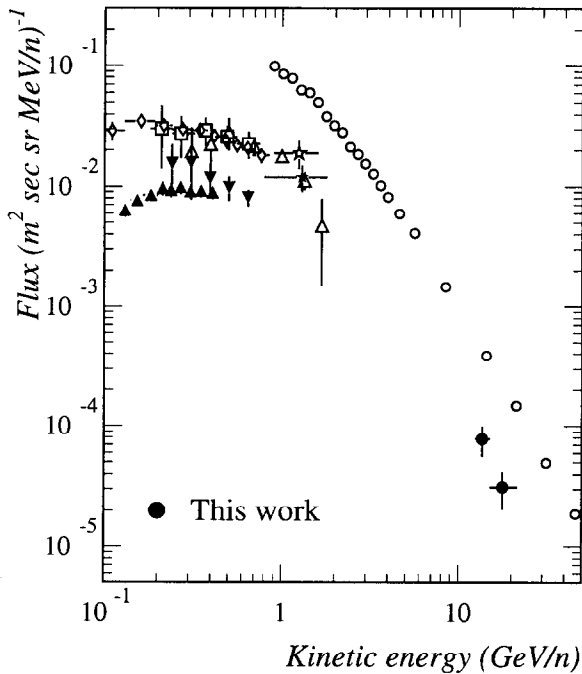


Figure 4. *Filled circles*: ^2H flux measured by CAPRICE98. *Open circles*: He flux measured by CAPRICE98 (preliminary result). Other symbols: ^2H flux from different experiments. *Open diamonds*: AMS 98 [14]; *open squares*: BESS 93 [15]; *open triangles*: CAPRICE94 [13]; *open star*: Bogomolov et al. [9]; *filled star*: Bogomolov et al. [10]; *filled downward-pointing triangles*: MASS1 [12]; *filled upward-pointing triangles*: Webber et al. [11].

than protons, only events with $\theta_c < 40$ mrad were considered.

The RICH deflection resolution function is related to the angular resolution of the detector. This quantity was derived from ground muon data and used as input of a simulation. A large sample of proton events was generated according to the observed all-particle spectrum, the RICH response simulated and the RICH deflection resolution function constructed on an event-by-event basis.

To determine the spectrometer resolution func-

tion we fitted the experimental distribution of the variable $\eta - \eta_{RICH}$ with a function obtained by convolving the RICH deflection resolution function with a Lorentian function, whose parameters were left free to vary. The solid line in fig.3 (right plot) represents the results of the fitting procedure. For this purpose, only events in the shaded area of this figure were used for the fit in order that the deuteron component does not alter the result. We took a Lorentian function with the parameters obtained by the fit as the best estimate of the spectrometer resolution function.

3.4. Proton and deuteron component in the spectrometer

We generated a large sample of both protons and deuterons according to the observed all-particles spectrum. For each event the RICH signal was generated according to P_{OFF} and the deflection smeared according to the high energy spectrometer resolution function.

From the simulation we obtained the proton contamination and the deuteron selection efficiency. These quantities were used to estimate the number of protons and deuterons in the spectrometer.

Fig. 1 shows the simulated background distribution (shaded area) together with the number of selected events as a function of the rigidity. As we can see the proton background dominates the sample up to ~ 25 GV. With the increasing rigidity, the deuteron component emerges from the background, which reaches its minimum ($\sim 28\%$ of the selected events) between 32 and 40 GV.

4. The ^2H flux and the $^2\text{H}/\text{He}$ ratio

In order to derive the flux of ^2H at the top of the atmosphere the number of events in the spectrometer were corrected for the total detection efficiency, for the geometrical acceptance of the instrument and for the attenuation and the secondary production due to interactions in the material above the tracking system, including the residual atmosphere (5.5 g cm^{-2}). See reference [7] and references therein for more details.

Fig. 4 shows the ^2H flux measured by CAPRICE98 compared with the results coming

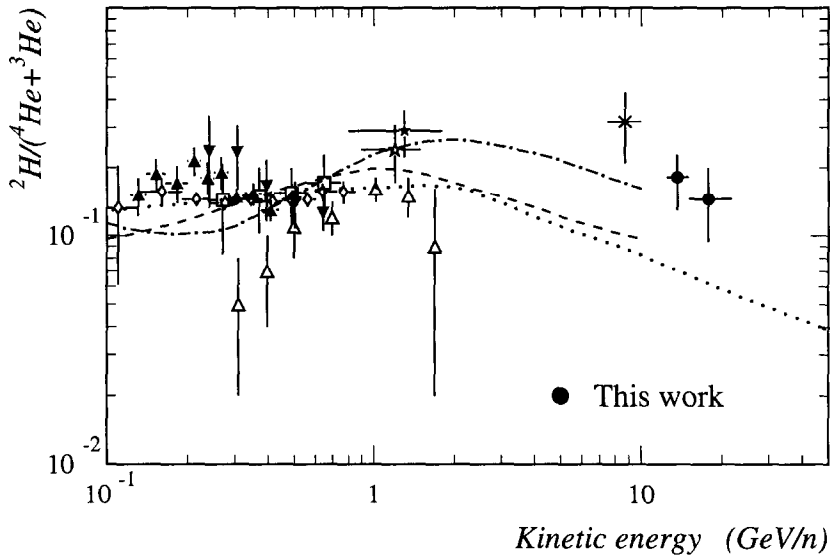


Figure 5. ${}^2\text{H}/\text{He}$ ratio. *Filled circles*: CAPRICE98 result. *Asterisk*: results from Apparao et al. [8]. Other symbols: same as fig. 4. Curves: theoretical predictions on the basis of the Leaky-Box Model. *Dotted curve*: Stephens [17]; *dashed curve* Webber [18]; *dotted-dashed curve*: Mewaldt et al. [16].

from other experiments. In the same plot the He flux measured by CAPRICE98 is also shown (open circles). All the existing data on the ${}^2\text{H}$ flux are below 2 GeV/n, where the solar modulation strongly affects the cosmic-ray flux. The CAPRICE98 measurement represents the first result obtained at energies above ~ 2 GeV/n.

At high energy the ${}^2\text{H}$ is mainly a product of the nuclear interactions of primary cosmic-ray He with the interstellar medium. The ${}^2\text{H}/\text{He}$ ratio is thus a meaningful quantity to study the interstellar propagation mechanism for cosmic-ray He.

Fig. 5 shows the ${}^2\text{H}/\text{He}$ ratio measured by CAPRICE98 compared with the results coming from other experiments. It may be pointed out that all measurements plotted in fig. 5, except for those from AMS98, were carried out using balloon-borne instruments. As a consequence the results have been corrected for the atmospheric attenuation and secondary production. The atmospheric production is particularly significant for the ${}^2\text{H}$ measurements due to the large amount

of deuterons produced during the fragmentation of air nuclei. This contribution, which increases at decreasing energy, is difficult to estimate, so that the low energy balloon data are affected by large systematic uncertainties. This could partly explain the observed disagreement among low energy data in fig. 5. Below ~ 1 GeV/n the ${}^2\text{H}/\text{He}$ ratio is also affected by solar modulation. The general trend is that a higher solar modulation level corresponds to a larger value of the ${}^2\text{H}/\text{He}$ ratio. Above ~ 1 GeV/n the solar modulation effect is indeed small. Besides the CAPRICE98 result, only one measurement exist above 2 GeV/n [8]. The two results are consistent, within the experimental errors.

The general agreement is that cosmic-ray H and He have the same propagation history of heavier cosmic-ray nuclei. The standard propagation models for light nuclei assume in fact the same amount of matter traversed within the Galaxy as deduced from the study of the most abundant heavier secondary cosmic-ray nuclei.

In fig. 5 the experimental results on the $^2\text{H}/\text{He}$ ratio are compared with some theoretical predictions. All the three calculations have been carried out on the basis of standard models formulated within the framework of the Leaky-Box Model. To interpret the experimental observation below ~ 1 GeV/n assumptions on the solar modulation mechanism and on the solar activity level are also necessary. Both the calculations from references [16,17] refer to minimum solar activity, whereas that from reference [18] assume an intermediate modulation level.

By comparing the theoretical predictions at high energy it follows that, even within the same standard interstellar propagation scenario, different calculations give results that differ by large amounts. The common feature is a broad peak in the $^2\text{H}/\text{He}$ ratio at about 1 GeV/n, above which the secondary-to-primary ratio decreases. This is a consequence of the decreasing escape mean free path from the Galaxy, as deduced from the abundances of heavy secondary cosmic-rays. The high energy data suggest a better agreement with the result of Mewaldt et al. [16].

5. Conclusion

In the CAPRICE98 experiment, a gas RICH was flown for the first time with a magnet spectrometer for the study of cosmic rays. Using the RICH as a threshold device it was possible to separate ^2H from ^1H in the energy range from 12 to 22 GeV/n. Moreover the instrument configuration allowed to parameterize the spectrometer response at float by using the deflection information of the RICH. The result was then used to simulate the proton background and the deuteron selection efficiency.

If we exclude the measurement of Apparao et al. [8], the new results given by the CAPRICE98 experiment, concerning both the ^2H flux and the $^2\text{H}/\text{He}$ ratio, represent the only experimental data on the ^2H abundance above 2 GeV/n. By comparing the CAPRICE98 results with some theoretical predictions it follows the data can be interpreted in the framework of the standard scenario, which assumes for H and He the same propagation history of heavier cosmic-ray nu-

clei. However any definitive conclusion cannot be drawn, due to the paucity of high energy measurements and to the uncertainties on the propagation parameters, which lead to disagreements even within the same model.

REFERENCES

1. M. Hof et al., NIM A 345 (1994) 561
2. R.L. Golden et al., NIM A 148 (1978) 179
3. R.L. Golden et al., NIM A 306 (1991) 366
4. M. Ricci et al., Proc.26th ICRC 5 (1999) 49
5. M. Boccioni et al., NIM A 370 (1996) 403, M. Ricci et al., Proc.26th ICRC 5 (1999) 49
6. D. Bergström et al., NIM A 463 (2001) 161
7. E. Vannuccini, PhD thesis, Florence University (Italy)
8. K.M.V. Apparao et al., Proc.13th ICRC 1 (1973) 126
9. E.A. Bogomolov et al., Proc.16th ICRC 1 (1979) 330
10. E.A. Bogomolov et al., Proc.24th ICRC 2 (1995) 598
11. W.R. Webber et al., ApJ 380 (1991) 230
12. P. Papini, PhD thesis, Florence University (Italy)
13. N. Finetti, PhD thesis, Perugia University (Italy)
14. G. Lamanna et al., Proc.27th ICRC (2001) 1614
15. J. Z. Wang et al., ApJ 564 (2002) 244
16. R. A. Mewaldt et al., AIP Conf. Proc. 183 (1989) 124
17. S. A. Stephens, Adv.Sp.Res. 9 (1989) 145
18. W. R. Webber, Adv.Sp.Res. 5 (1997) 755